01 Jan 1993

A New Technique to Decompose Closely Spaced Interface and Bulk Trap States using Temperature Dependent Pulse-Width Deep Level Transient Spectroscopy Method: An Application to PT/CdS Photodetector

C. W. Wang

Cheng-Hsiao Wu
Missouri University of Science and Technology, chw@mst.edu

Jack L. Boone
Missouri University of Science and Technology

Recommended Citation

C. W. Wang et al., "A New Technique to Decompose Closely Spaced Interface and Bulk Trap States using Temperature Dependent Pulse-Width Deep Level Transient Spectroscopy Method: An Application to PT/CdS Photodetector," *Journal of Applied Physics*, vol. 73, no. 2, pp. 760-766, American Institute of Physics (AIP), Jan 1993.
The definitive version is available at https://doi.org/10.1063/1.353334

A new technique to decompose closely spaced interface and bulk trap states using temperature dependent pulse-width deep level transient spectroscopy method: An application to PT/CdS photodetector

C. W. Wang, C. H. Wu, and J. L. Boone
Department of Electrical Engineering, University of Missouri-Rolla, Rolla, Missouri 65401

(Received 15 June 1992; accepted for publication 28 September 1992)

A novel method is presented here to experimentally decompose nonexponential capacitive transients into the appropriate components from the closely spaced deep trap states. Using temperature dependent pulse-width deep level transient spectroscopy (TDP-DLTS) technique, we show for the first time that two bulk trap states and one continuously distributed interface states in (Pt/CdS) photodiodes can be successfully separated. The basic principle is to set the applied pulse width to follow an averaged temperature-dependent capture time constant and divide the DLTS spectrum. In the example of Pt/CdS photodiodes, we show that all physical parameters including thermal activation energies, capture cross sections, and trap densities are more accurately calculated after each component is separated from others. The origins for those bulk traps and interface states are also discussed. Without any complicated mathematics or program, TDP-DLTS can be applied to both large and small voltage pulse DLTS measurements.

I. INTRODUCTION

Over the past three decades, CdS has been the subject of considerable interest because of its potential use in photovoltaic applications. As is well-known, deep defect levels in the band gap play a major role in determining the performance of devices. However, in contrast to Si, GaAs, and related compounds, very few papers on the characterization of deep trap levels of CdS samples have been published. Furthermore, to our knowledge, there have been very limited reports[1] on the simultaneous measurements of both bulk and interface states on CdS Schottky diodes.

A number of techniques for interface-state measurement have been proposed, including the quasistatic C–V method,[2,3] the Gary–Brown technique,[4] the conductance technique,[5–7] and deep level transient spectroscopy (DLTS).[8] Only the latter two techniques can yield information on the cross section. DLTS, originally developed for characterization of bulk traps, has been applied to the measurement of interface states.[9–14] Unlike the conductance technique, the transient capacitance measurement is independent of the surface potential fluctuation in metal oxide semiconductor (MOS) structures.[15]

In the traditional DLTS technique, the activation energies, capture cross sections, and concentration of the bulk traps can be accurately determined when those traps are well-separated in energy. On the other hand, interface states can be determined by using the energy-resolved DLTS method.[13,16–18] In this method one applies a small pulse voltage with an amplitude of only several kT, and a long fixed filling pulse to the devices during the capture process is used. However, whenever the trap energy levels are close to each other, the transient signals from those traps are nonexponential and the mathematical analysis of the DLTS signals is always subject to error. In such situations, a correlation method should be used to extract each elementary signal and to estimate its parameters. The method of moments,[19] which can provide high energy resolution when a multiexponential is encountered, was applied to DLTS measurements by Kirchner *et al.*[20] It has the serious disadvantages of being iterative and baseline sensitive, and it assumes no truncation errors caused by finite measurement times. The modulating function method[21] has been applied to DLTS measurements[22] to eliminate these drawbacks. The DLTFS method[23] has also been proposed to solve the overlapping of two exponential functions by using the discrete Fourier transformation on the digitalized capacitance–time transients. Here, we would like to point out that all of the above methods can only be applied to discrete energy-level measurements, such as bulk trap measurements, and not to interface-trap measurements. Quite recently, Dmowski[24] presented a multipoint correlation method which, strictly speaking, is a signal processing method where the input signal is multiplied by a reference signal (usually called a "weighting" function), and the product is filtered by a linear sampled data filter.[25] Although his method could be used to separate bulk traps and interface states from the overlapping DLTS spectrum, no real experimental results were shown in his report. Furthermore, we find his method relies on too complicated mathematical calculations, especially when high selectivity is needed.

In this paper, we develop a new DLTS technique in which the pulse-width closely follows the capture time constant of an assumed or averaged deep trap. Since the capture time constant of electron is a function of temperature, it is essential to let the injection pulse width t_p change with temperature instead of keeping it at a fixed pulse width during the capture process as in conventional DLTS measurements. Here, we will show that temperature dependent pulsewidth-DLTS (TDP-DLTS) technique is capable of separating closely spaced traps (for both bulk traps and interface states). If we set the injection pulse width to

 0021-8979/93/020760-07$06.00

follow right on the capture time of a "concentration-averaged" trap level due to two closely spaced traps, the DLTS signal obtained will have a contribution only from the shallower one of the two. This is because when the capture time constant of the deeper trap is longer than the time duration of the applied pulse, very few electrons have been captured with respect to that trap level and hence the absence of the corresponding DLTS signal. The fact that a saturation of the DLTS signal for the shallower trap component can be obtained if the pulse width follows the capture time constant of an averaged trap level can be verified as we will show later. After subtracting the saturated DLTS signal of the shallower trap from the total DLTS signal, we can then obtain the corresponding one for the deeper trap. Thus, here we present an experimental decomposition method in contrast with those mathematical methods mentioned earlier. We will also show that this method of "follow-the-capture-time-constant-of-an-averaged-trap-level" and divide the trap levels can be repeated. In our samples, two deep electron bulk traps and a broad distribution of interface states are successfully decomposed using this technique. This is shown in Sec. III. In Sec. II, we describe briefly our measurement principles. The conclusion is in Sec. IV.

II. MEASUREMENT PRINCIPLES

A. Traditional DLTS (large voltage pulse)

Consider a MOS diode with an n-type substrate. When the bulk trap is located above the midgap, the capacitance transient $\Delta C=[C(t_2)-C(t_1)]$ under conventional DLTS measurement by applying a forward injection pulse with reverse quesient bias voltage V_r, pulse voltage V_p and pulse width t_p, can be reduced to [26]

$$\Delta C=-S(g_e)\frac{C(t_1)^3}{\epsilon_s N_D(w)}\int_{y_p}^{y(t_1)}\left(\frac{1}{C_{\rm ox}}+\frac{x}{\epsilon_s}\right)N_T(x)dx, \tag{1}$$

where $S(g_e)=\exp(-g_e t_2)-\exp(-g_e t_1)$, ϵ_s is the permittivity of semiconductor material, w is the depletion layer depth, $C_{\rm ox}$ is the oxide capacitance per unit area, N_D is the shallow donor density, N_T is the trap density, y_p and y are the characteristic depths where the bulk trap level crosses the Fermi level at the end of the capture process and in the emission process, respectivity. Since the emission rate, g_e, depends exponentially on temperature according to the relation [27]

$$g_e=\sigma_n V_{\rm th} N_c \exp[-(E_c-E_{\rm bt})KT], \tag{2}$$

the correlation signal, ΔC, goes through a maximum at the temperature $T_{\rm max}$, where the emission rate is related to the sampling time as follows:

$$g_e=\ln(t_2/t_1)/(t_2-t_1). \tag{3}$$

The bulk trap energy level ($E_{\rm bt}$) and the capture cross-section at infinite temperature (σ_∞) can be calculated from the Arrhenius plot of the emission rates obtained from a series of temperature scans for different t_1 and t_2 values. The spatial distribution of the bulk trap density can be evaluated as outlined in Ref. 26.

B. Energy-resolved DLTS (small voltage pulse, $V_p-V_r<0.1$ V)

The energy-resolved DLTS technique is specially designed for analyzing the interface states in MOS devices. When the injection pulse height is small enough, the DLTS signal coming from the interface states within the very narrow interval (E_r, E_p) is a rather sharp spectrum. This behavior is one of the characteristic features of a quasi-discrete level localized at the energy $E_t\simeq(E_r+E_p)/2$. In this situation, the ΔC that comes from the interface states can be reduced to[14,26]

$$\Delta C=\frac{-C(t_1)^3}{\epsilon_s N_D(w)}\frac{KT}{C_{\rm ox}}N_s(E_t)\ln\left(\frac{t_2}{t_1}\right) \tag{4}$$

which is the same expression as for a discrete level.[28] Furthermore, the activation energy of the interface state ΔE_t can be evaluated using the method in Ref. 13.

In many cases, the capture cross-section is expressed as $\sigma_n=\sigma_\infty\exp(-\Delta E_\infty/KT)$, where σ_∞ and ΔE_∞ are constants inherent to the level.[29] Therefore, we assume that surface states at different energies have different σ_∞ and ΔE_∞,

$$\sigma_n(E_t,T)=\sigma_\infty(E_t)\exp[-\Delta E_\infty(E_t)/KT]. \tag{5}$$

In addition, the emission time constant τ_e versus temperature relation can be written as,[13]

$$\frac{\tau_e}{\sqrt{T}}=\left[\sqrt{\frac{3K}{m^*}}N_D\sigma_\infty(E_t)\times\exp\left(-\frac{\Delta E_\infty(E_t)+qV_s-1/2\Delta E_F}{KT}\right)\right]^{-1}. \tag{6}$$

Thus, the slope of $\ln(\tau_e/\sqrt{T})$ vs $1/KT$ plot gives an apparent activation energy $\Delta E_\infty(E_t)+qV_s-1/2\Delta E_F$ and the energy-dependent term of the capture cross-section $\sigma_\infty(E_t)$ can be obtained as a function of E_t from the intersection with the $\ln(\tau_e/\sqrt{T})$ axis.

To deduce $\Delta E_\infty(E_t)$, we have to know $qV_s-1/2\Delta E_F$. The surface potential, qV_s, can be determined from the capacitance–voltage characteristics provided that the oxide capacitance and the doping density are known.[30]

C. Temperature dependent pulsewidth-DLTS (TDP-DLTS)

TDP-DLTS is an experimental method to decompose any overlapping spectrum in traditional and energy-resolved DLTS measurements. No *a priori* mathematics are needed. The essence of TDP-DLTS technique is to provide an injection pulse width that is directly proportional to the capture time constant of an averaged trap level and to locate the saturated peak of the shallower component first from the overlapping DLTS spectrum. The decomposition can be made by subtracting the shallower saturated peak from the total overlapping one. All physical parameters of the separated trap including ther-

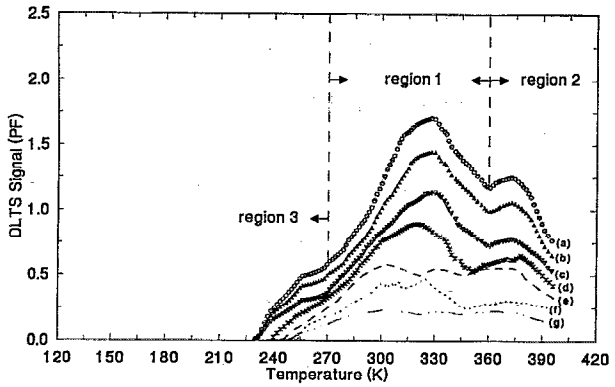

FIG. 1. DLTS signals of Pt/CdS photodetectors at different pulse width (t_p) conditions. (a) $t_p=100$ ms, (b) $t_p=10$ ms, (c) $t_p=1$ ms, (d) $t_p=100\ \mu$s, (e) $t_p=10\ \mu$s, (f) $t_p=1\ \mu$s, and (g) $t_p=0.1\ \mu$s $V_r=-3$ V, and $V_p=0$ V.

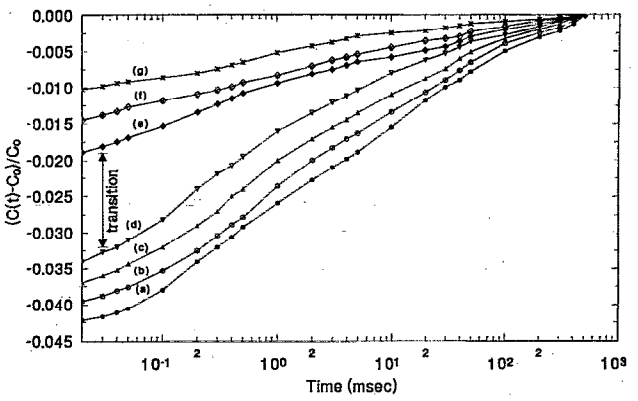

FIG. 2. Capacitance transients after different constant capture pulse-widths were turned off at $T=320$ K. (a) $t_p=100$ ms, (b) $t_p=10$ ms, (c) $t_p=1$ ms, (d) $t_p=100\ \mu$s, (e) $t_p=10\ \mu$s, (f) $t_p=1\ \mu$s, and (g) $t_p=0.1\ \mu$s. C_o is the baseline, $V_r=-3$ V, and $V_p=0$ V.

mal activation energy, capture cross-section, and trap density can be more accurately calculated.

III. EXPERIMENTAL RESULTS AND DISCUSSION

The experimental results were from samples of Pt/CdS Schottky barrier diodes provided by Eagle Picher Research Laboratory in Miami, Oklahoma. These are planar devices which have been designed for use as photodetectors operating in the photovoltaic mode. Generally, the devices display a large reverse breakdown voltage and the cut-in voltage is about 0.6 V. Reverse currents (dark) are around 1 μA per cm^2 and the potential barrier is near 1 eV. The measurements were made on approximately 30 devices most of which displayed "normal" characteristics to the observations reported here.

The upper limit of the temperature for the DLTS experiments has been set at 395 K to avoid any irreversible sample alteration. Typical large pulse DLTS measurements under different pulse widths, t_p, are shown in Fig. 1. Saturation of the spectrum is reached whenever $t_p \geqslant 100$ ms. In Fig. 1, we observe the obvious overlapping peaks when $t_p \geqslant 10\ \mu$s. From the saturated peak ($t_p=100$ ms), we note that there are three DLTS peaks located at three different temperature regions; region 1 between 270 to 360 K, region 2 greater than 360 K, and region 3 below 270 K. To decompose the whole spectrum, we need to know the number of subpeaks and to roughly estimate the "averaged" capture time constant from the combined components first. Figure 2 shows the emission capacitance transient from different capture pulse widths at temperature $T=320$ K which is somewhere within region 1 as shown in Fig. 1. A clear transition jump between 100–10 μs can be found in this figure. Thus, if we set the capture time t_p near to 100 μs, the shallower trap should be almost filled by electrons while the deeper one is almost empty. In Fig. 3 we show that when temperature is at the boundary of two overlapping regions, there exist two transitions. The transition jumps for the larger pulse width (transition 2) and for the smaller one (transition 1) are corresponding to the average capture time constant of the deeper and the shallower traps at that temperature, respectively. Therefore, by scanning the whole temperature range, two roughly estimated capture time constant curves can be established. This is shown in Fig. 4. In Fig. 4, τ_a and τ_b are the estimated averaged capture time constants of DLTS peaks at region 3 and region 1 plus region 3, respectively. Thus, if we set the capture pulse width, t_p, to follow the τ_a curve of Fig. 4, the DLTS signal obtained will be the low temperature (region 3) DLTS peak only with very few contributions from region 1. Similarly, if t_p is set to follow the τ_b curve of Fig. 4 we will obtain the DLTS signal from the low and the middle temperature peaks only. Hence, a pure DLTS signal from region 1 (or pure peak 1) can be separated by subtracting the pure peak 3 (which is the peak obtained from t_p that follows the τ_a curve) from the saturated overlapping peaks due to region 1 plus region 3 (obtained from t_p that follows the τ_b curve). Similarly, we can decompose a pure peak 2 by subtracting the saturated overlapping peaks due to region 1 plus region 3 from the total

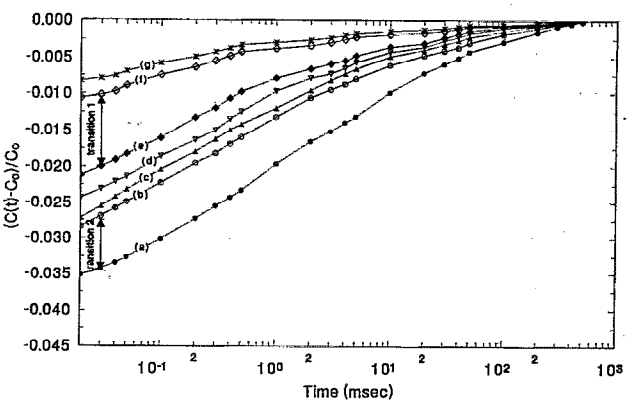

FIG. 3. Capacitance transients after different constant capture pulse-widths were turned off at $T=270$ K. (a) $t_p=100$ ms, (b) $t_p=10$ ms, (c) $t_p=1$ ms, (d) $t_p=100\ \mu$s, (e) $t_p=10\ \mu$s, (f) $t_p=1\ \mu$s, and (g) $t_p=0.1\ \mu$s. C_o is the baseline, $V_r=-3$ V, and $V_p=0$ V.

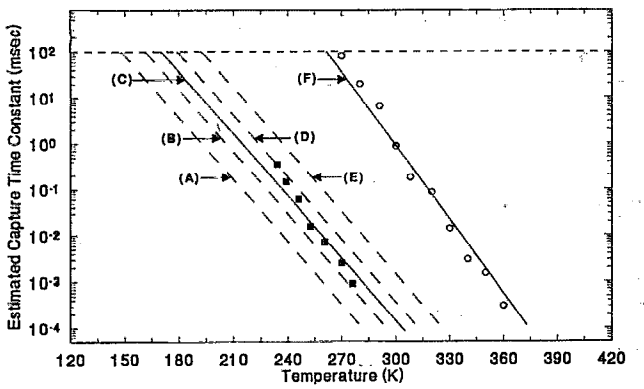

FIG. 4. Two estimated averaged capture time constant curves in different temperature regions, τ_a (for region 3 in Fig. 1) and τ_b (for region 3 plus region 1 in Fig. 1). The injection pulsewidth curves that follow the τ_a with different multipliers m; (A) 0.1 τ_a, (B) 0.4 τ_a, (C) τ_a, (D) 2.5 τ_a and (E) 10 τ_a. The solid square (■) data points are for log $(\tau_a) \approx 0.0450 \times T + 9.651$ and the hollow circle data points (○) are for log $(\tau_b) \approx -0.0533 \times T + 15.93$.

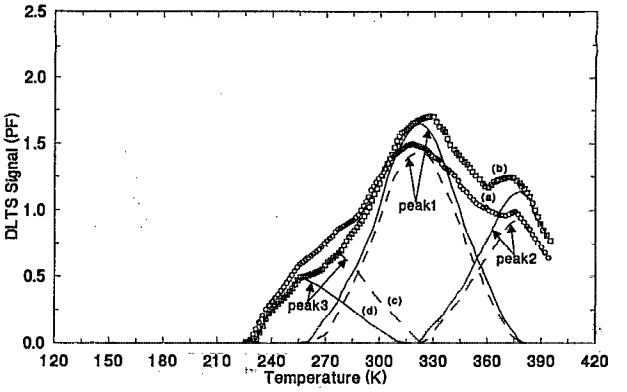

FIG. 6. DLTS signals for constant capture pulsewidths under different biased voltages as well as their decompositions by TDP-DLTS; (a) DLTS signal for $V_r = -6$ V and $V_p = -3$ V, (b) DLTS signal for $V_r = -3$ V and $V_p = 0$ V, (c) the decomposition of curve (a), and (d) the decomposition of curve (b). The decomposed pure peaks 1 and 2 show fixed peak temperatures; however, the peak temperature of pure peak 3 shows a shift under different bias voltage. Note that without our proper decompositions, errors can be easily made in locating the peak temperatures as shown in this figure.

DLTS spectrum (which is obtained by t_p keeping a constant, 100 ms). As a result, well-separated DLTS signals from different trap levels at different temperature ranges can be obtained. To verify this conclusion, we show first how we get the pure peak 3 by TDP-DLTS. We set the pulse width t_p at a maximum value of 100 ms beginning at the low temperature range and then follow the capture time constant of the τ_a curve in five different multipliers. The proportionality constant m, at $m=0.1$ (case A), 0.4 (case B), 1 (case C), 2.5 (case D), and 10 (case E) is shown in Fig. 4. The TDP-DLTS measurement results under these five kinds of capture pulse widths are shown in Fig. 5. We show that when the pulse width follows a smaller multiplier (such as $m=0.1$ and 0.4) the peak 3 shows a partially filled peak. At $m=1$, peak 3 reaches a saturated height. When $m>1$, the DLTS peak becomes broader with increasing multipliers. Thus, the pure peak 3 is curve C which has a saturated height without a broadening effect from peak 1. Similarly, we can obtain a saturated height of peak 3 plus peak 1 without a broadening effect from peak 2. We must emphasize that the TDP-DLTS technique does not require the pulse width t_p to follow precisely on the real curve of the capture time constant. Here we show that it is good enough to obtain the saturated peak without a broadening effect and accurately locate the peak temperature by setting t_p somewhere between $0.5\tau_a$–$2\tau_a$. The decomposition results under different applied bias voltages are shown in Fig. 6.

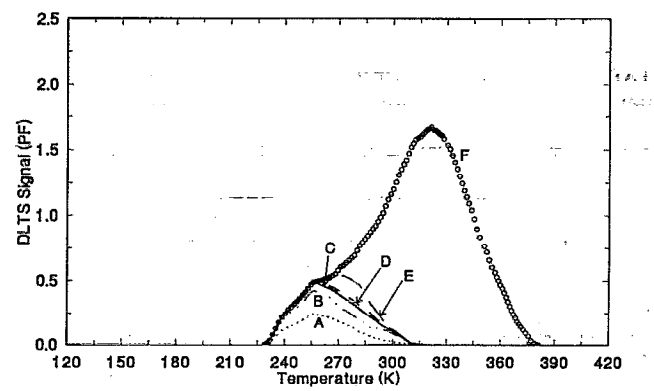

FIG. 5. TDP-DLTS signals measured with pulse widths which parallel the capture time constants τ_b and τ_a as functions of temperature. Five different curves are shown corresponding to (a) $t_p \approx 0.1\tau_a$, (b) $t_p \approx 0.4\tau_a$, (c) $t_p \approx \tau_a$, (d) $t_p \approx 2.5\tau_a$, (e) $t_p \approx 10\tau_a$, and (f) $t_p \approx \tau_b$. In each case, the maximum t_p is 100 ms. Curves (c) and (f) can be shown to be the complete DLTS signals from region 3 and region 3 plus region 1, respectively. $V_r = -3$ V and $V_p = 0$ V.

In Fig. 6, we show that the locations of peak temperatures of pure peak 1 and peak 2 are almost fixed even though different pulse voltages were applied. However, pure peak 3 has the peak temperature shifted under different pulse voltages. This is due to the fact that[14,26] the measured energy position of the interface states depends on the bias voltage. As a result the peak temperature is shifted. However, the peak temperatures of bulk traps are fixed with respect to the bias voltage. Therefore, we can conclude that pure peak 1 and peak 2 are bulk traps, but pure peak 3 is the interface states. To confirm this judgement further, we use the energy-resolved DLTS at different reverse quesient bias voltage V_r while keeping the same pulse amplitude ($\Delta V_p = 50$ mV). The results are shown in Fig. 7. Figure 7 clearly proves that peak 3 is indeed the interface states because the peak temperature shifts towards the higher temperature with increasing V_r. Another meaningful result shown in Fig. 7 is that the amplitude of peak 3 (interface states) increases with increasing reverse bias voltage V_r; however the bulk traps, peak 1 (E_{bt1}) and peak 2 (E_{bt2}), are the opposite. It implies qualitatively that both bulk traps have decreasing density with increasing distance from the interface, and the interface states have increasing density with deeper state energy.

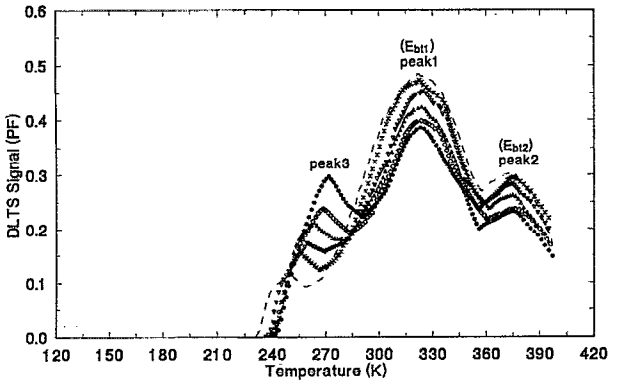

FIG. 7. Energy-resolved (small voltage pulse) DLTS signals under different biased voltage conditions; ●, $V_r=-7$ V and $V_p=-6.15$ V; ○, $V_r=-6$ V and $V_p=-5.95$ V; ▲, $V_r=-5$ V and $V_p=-4.95$ V; ▽, $V_r=-4$ V and $V_p=-3.95$ V; *, $V_r=-3$ V and $V_p=-2.95$ V; and ---, $V_r=-2$ V and $V_p=-1.95$ V. ▽ $V_p=50$ mV and $t_p=100$ ms.

All physical parameters of the bulk traps, including activation energies, capture cross-sections, and trap densities, can be accurately calculated after the decomposition is made using related Eqs. (1)–(3) and related equations given in the references. The results are shown in Figs. 8 and 9, respectively. A summary of our results and comparison with those of other authors are shown in Table I. In Ref. 33, Claybourn and his co-workers have reported that the E_{bt1} peak always appears in the annealed samples of vapor-phase-grown single-crystal CdS, which is not found in the as-grown samples. Furthermore, using scanning electron microscopy, they observed a clear array of subgrain boundaries in the annealed samples when compared those with as-grown ones. They finally concluded that dislocations might aggregate to form subgrain boundaries by a dislocation polygonization process, as has also been observed to occur in single crystals of CdTe.[37] Therefore, the DLTS response is from those dislocations which can be expected to produce a deep-lying state in the energy gap

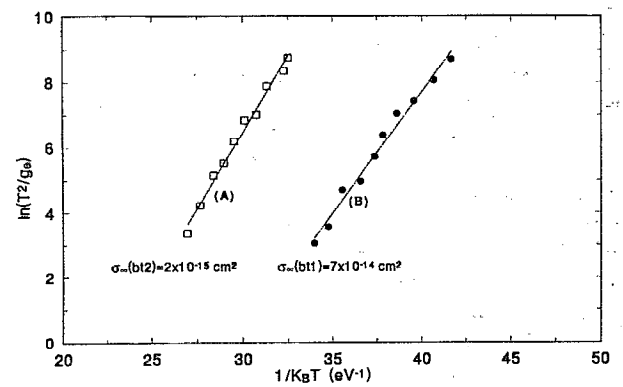

FIG. 8. Arrhenius plots for temperature dependent emission rates of decomposed pure bulk electron traps. For (A) $E_{bt1}=0.934$ eV and $\sigma_\infty(bt2)=2\times10^{-15}$ cm^2; for (B) $E_{bt1}=0.746$ eV and $\sigma_\infty(bt1)=7\times10^{-14}$ cm^2. The capture cross-sections σ_∞ were obtained by extrapolation.

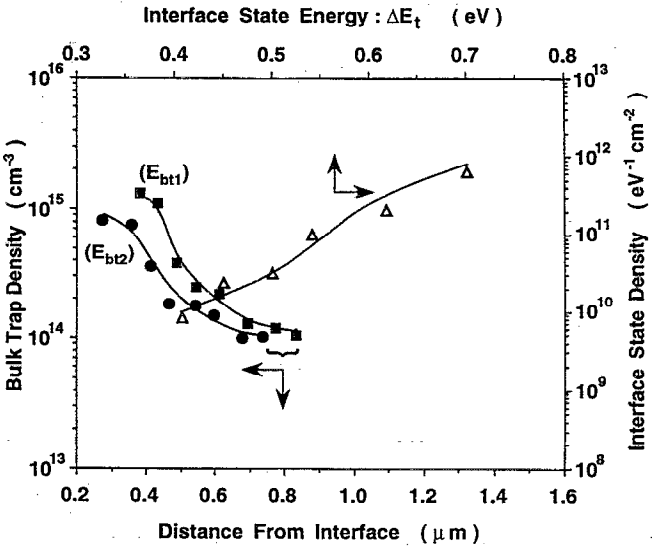

FIG. 9. Spatial distribution of the bulk trap densities and the interface state densities as determined by TDP-DLTS and energy-resolved DLTS, respectively.

and is capable of accepting/re-emitting carriers from/to the free carrier bands. The DLTS signals due to dislocations in Si and Ge materials have also been reported in Refs. 38–41. For the E_{bt2} trap, Housin and his co-workers in Ref. 36 suggested that this could be the "X centers" and probably correlated with cadmium vacancies, although the microscopic description of the associated defect for the X centers and their fundamental contribution to the persistent photoconductivity of undoped CdS crystal[42] are still not clear.

From energy-resolved ($\Delta V_p=50$ mV)DLTS measurements, the $\Delta E_\infty(E_t)$ and $\sigma_\infty(E_t)$ of the interface states as functions of E_t can be obtained, which are shown in Fig. 10. The interface state density, $N_s(E_t)$, is calculated and given in Fig. 9. From Fig. 9, we find the interface state density increases with state energy ΔE_t increasing. This

TABLE I. Physical characteristic parameters of E_{bt1} and E_{bt2} electron traps from DLTS measurement in Pt/CdS devices obtained in this work and comparisons to others.

	CdS bulk electron trap			
	E_{bt1}		E_{bt2}	
Ref.	Activation energy (eV)	Electron capture cross-section σ_∞ (cm^2)	Activation energy (eV)	Electron capture cross-section σ_∞ (cm^2)
This work	0.746	7×10^{-14}	0.934	2×10^{-15}
31	0.75	10^{-12}–10^{-14}		
32	0.735	1.2×10^{-16}		
33	0.74	3×10^{-15}		
34	0.725	1×10^{-12}		
1			0.925	5×10^{-15}
35			0.92	5×10^{-13}
36			0.93	5×10^{-15}

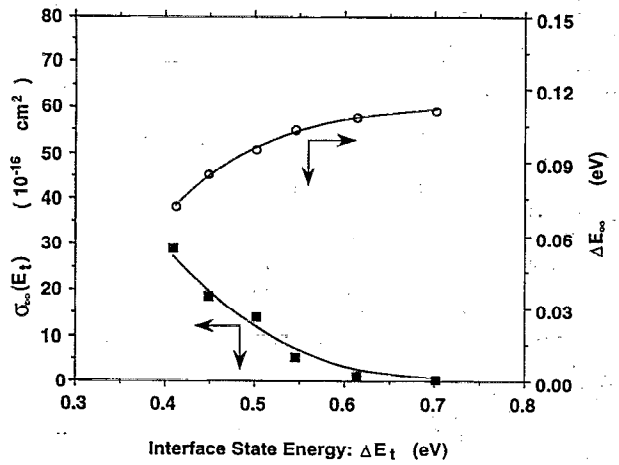

FIG. 10. Energy-dependent electron capture cross section σ_∞ and capture barrier ΔE_∞.

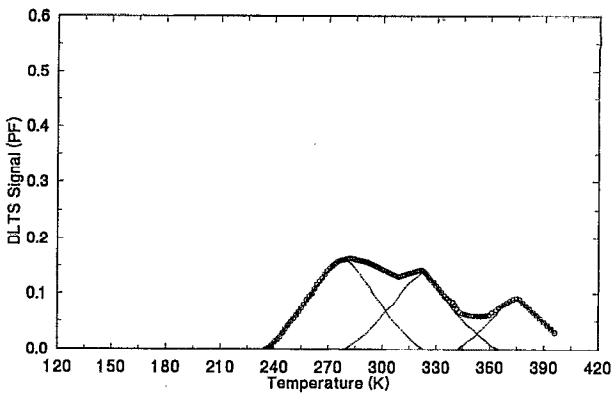

FIG. 11. The overlapping peaks of small voltage pulse DLTS measurements from the "abnormal" samples. In this figure, the open circles (○) correspond to the DLTS signal and the solid line is the decomposition curve. $V_r=-7$ V, $V_p=-6.95$ V, $\Delta V_p=50$ mV, and $t_p=100$ ms.

result is consistent with previous reports[43,44] that oxygen adsorption on the CdS surface produces a broad continuous distribution of surface states with a peak centered at $E_c-E_t\cong 0.8$ eV.

From our calculations, we note that ΔE_∞ of the interface states in our samples are all positive. A theoretical model that accounts for the positive ΔE_∞ is lattice relaxation multiphonon emission (MPE)[45–47] which has been proposed to explain the temperature variation of the capture cross-section of bulk traps in GaAs and GaP (Refs. 29 and 48) and also for interface states in Si/SiO_2 MOS structures.[9,11] This model assumes a neutral center in which vibrations of a single lattice coordinate linearly modulate the depth of the potential well binding the carrier. For sufficiently large vibrations at high temperatures, the level can cross into the conduction band and capture an electron. Immediately after capture, the lattice equilibrium position changes leaving the captured carrier in a highly excited vibrational state which rapidly decays by multiphonon emission into the equilibrium state. Our experimental results suggest that those interface states in Pt/CdS photodiodes are in agreement with the multiphonon emission capture model.

In our experiments, we have some "abnormal" devices which have smaller cut-in voltage (around 0.4 V only) than that of the standard ones. We found for those abnormal samples, the overlapping peaks of the large voltage pulse DLTS measurements are similar as in those of standard ones; however, the small voltage pulse (energy-resolved) DLTS measurements show that obvious overlapping peaks in those abnormal samples, which is shown in Fig. 11. In Fig. 11, we also show that for such a small overlapping spectrum, the decomposition still can be easily done by TDP-DLTS method.

IV. CONCLUSIONS

A newly developed technique is presented here for separating overlapping DLTS spectrum from Pt/CdS photodetectors into two bulk electron traps and a band continuously distributed interface states. The basic principle of this technique is to set the applied pulse width to follow the temperature-dependent capture time constant of a "concentration-averaged" trap level and divide the spectrum. This method is reported here for the first time. We note that this method is very accurate even if the capture time constant of the averaged trap level is roughly estimated. This experimental decomposition method has the advantage of not using any mathematical programs proposed by many others.

Using the TDP-DLTS method, we first obtain the pure-lowest-temperature DLTS peak (peak 3 of the interface states). Then we can proceed to separate the pure-middle-temperature peak (peak 1 of the bulk trap) as well as the pure-highest-temperature peak (peak 2 of the bulk trap) from the total DLTS spectrum. The activation energies, capture cross-sections, and trap densities of the bulk traps can be more accurately calculated after they are well-separated using large voltage pulse measurements. We conclude that the possible origins for E_{bt1} (peak 1) and E_{bt2} (peak 2) are deep states associated with the dislocation and "X centers," respectively.

The physical parameters of the interface states have also been determined by using energy-resolved ($\Delta V_p=50$ mV) DLTS measurements. The origin is most likely due to oxygen adsorption at the CdS–Pt interface as reported earlier by others.

Finally, we also show we can successfully decompose overlapping DLTS spectrum when very small voltage pulse is applied.

Note added in proof. It is found that our Pt/CdS Schöttky diode samples also have gold contacts deposited on the back side of the CdS wafer to form another Schöttky barrier. This fact explains the "abnormal samples" with small (0.4 V) cut-in voltages described in the text and the different interface peak indicated in Fig. 11.

[1] M. Housin, M. Fialin, G. Bastide, G. Sagnes, and M. Rouzeyre, J. Cryst. Growth **59**, 246 (1982).
[2] M. Kuhn, Solid-State Electron. **13**, 873 (1970).

[3] A. Goetzberger, E. Klausmann, and M. J. Schulz, CRC Crit. Rev. **6**, 1 (1976).
[4] P. V. Gray and D. M. Brown, Appl. Phys. Lett. **8**, 31 (1966).
[5] H. Deuling, E. Klausmann, and A. Goetzberger, Solid-State Electron. **15**, 559 (1972).
[6] G. Declerck, R. Van Overstraeten, and G. Broux, Solid-State Electron. **16**, 1451 (1973).
[7] E. H. Nicollian and A. Goetzberger, Bell. Syst. Tech. J. **46**, 1055 (1967).
[8] D. V. Lang, J. Appl. Phys. **45**, 3014 (1974).
[9] M. Schulz and N. M. Johnson, Solid-State Commun. **25**, 481 (1978).
[10] M. Schulz and N. M. Johnson, Appl. Phys. Lett. **31**, 622 (1977).
[11] T. J. Tredwell and C. R. Viswanathan, Solid-State Electron. **23**, 1171 (1980).
[12] K. L. Wang, J. Appl. Phys. **47**, 4574 (1976).
[13] T. Katsube, K. Kakimoto, and T. Ikoma, J. Appl. Phys. **52**, 3504 (1981).
[14] F. Murray, R. Carin, and P. Bogdanski, J. Appl. Phys. **60**, 3592 (1986).
[15] E. H. Nicollian and J. R. Brews, *MOS Physics and Technology* (Wiley, New York, 1982), p. 254.
[16] W. D. Eades and R. M. Swanson, J. Appl. Phys. **56**, 1744 (1984).
[17] K. Yamasaki and T. Sugano, Appl. Phys. Lett. **35**, 932 (1979).
[18] N. M. Johnson, J. Vac. Sci. Technol. **21**, 303 (1982).
[19] I. Isenberg and R. Dyson, Biophys. J. **9**, 1337 (1969).
[20] P. D. Kirchner, W. J. Schaff, G. N. Maracas, L. F. Eastman, T. I. Chappel, and C. M. Ranson, J. Appl. Phys. **52**, 6462 (1981).
[21] B. Valeur, Chem. Phys. **30**, 85 (1978).
[22] K. Dmowski and A. Jakubowski, Rev. Sci. Instrum. **60**, 3845 (1989).
[23] S. Weiss and R. Kassing, Solid-State Electron. **31**, 1733 (1988).
[24] K. Dmowski, J. Appl. Phys. **71**, 2259 (1992).
[25] G. L. Miller, D. V. Lang, and L. C. Kimerling, Annu. Rev. Mater. Sci. **7**, 377 (1977).
[26] K. Yamasaki, M. Yoshida, and T. Sugano, Jpn. J. Appl. Phys. **18**, 113 (1979).
[27] W. Schockley and W. T. Read, Phys. Rev. **87**, 835 (1952).
[28] D. V. Lang, J. Appl. Phys. **45**, 3023 (1974).
[29] C. H. Henry and D. V. Lang, Phys. Rev. B **15**, 989 (1977).
[30] A. S. Grove, B. E. Deal, E. H. Snow, and C. T Sah, Solid-State Electron. **8**, 145 (1965).
[31] M. Hussein, G. Lleti, G. Sagnes, G. Bastide, and M. Rouzeyre, J. Appl. Phys. **52**, 261 (1981).
[32] C. Grill, G. Bastide, G. Sagnes, and M. Rouzeyre, J. Appl. Phys. **50**, 1375 (1979).
[33] M. Claybourn, A. W. Brinkman, G. J. Russell, and J. Woods, Philos. Mag. B **56**, 385 (1987).
[34] M. Hussein, G. Bastide, G. Sagnes, M. Rouzeyre, H. Rufer, and D. Ruppel, Inst. Phys. Conf. Ser. **46**, 414 (1979).
[35] D. Verity, D. Shaw, F. J. Bryant, and C. G. Scott, Phys. Status Solidi A **78**, 267 (1983).
[36] M. Housin, M. Fialin, G. Sagnes, G. Bastide, and M. Rouzeyre, Physica **117B&118B**, 155 (1983).
[37] K. Durose, G. J. Russell, and J. Woods, J. Cryst. Growth **72**, 85 (1985).
[38] A. Ourmazd, Contemp. Phys. **25**, 251 (1984).
[39] W. Schroter and M. Seibt, J. Phys. (Paris) Colloq. **9**, C4-329 (1983).
[40] L. C. Kimerling and J. R. Patel, Appl. Phys. Lett. **34**, 73 (1979).
[41] V. V. Kevder, Osipyan, A. Yu, W. Schroter, and G. Zoth, Physica Status Solidi A **72**, 701 (1982).
[42] H. C. Whright, R. I. Downey, and J. R. Canning, Brit. J. Appl. Phys. D **2**, 1953 (1968).
[43] J. Lagowski, C. L. Balestra, and H. C. Gatos, Surf. Sci. **29**, 213 (1972).
[44] L. J. Brillson, Surf. Sci. **51**, 45 (1975).
[45] K. Huany and A. Rhys, Proc. Roy. Soc. London, Ser. A **204**, 406 (1950).
[46] E. P. Sinyavskii and V. A. Kovarskii, Sov. Phys. Solid State **9**, 1142 (1967).
[47] R. Englman and J. Jortner, Mol. Phys. **18**, 145 (1970).
[48] D. V. Lang and C. H. Henry, Phys. Rev. Lett. **35**, 1525 (1975).